ELSEVIER

Journal of Organometallic Chemistry 625 (2001) 77–85

Journal of Organometallic Chemistry

www.elsevier.nl/locate/jorganchem

Syntheses and reactions of coordinatively unsaturated silyl, aryl osmium(II) complexes and the crystal structures of $Os[Si(OEt)_3]R(CO)(PPh_3)_2$ and $Os[Si(OEt)_3]R(CO)_2(PPh_3)_2$ (R = phenyl or *o*-tolyl)

Markus Albrecht, Clifton E.F. Rickard, Warren R. Roper *, Alex Williamson, Scott D. Woodgate, L. James Wright

Department of Chemistry, The University of Auckland, Private Bag 92019, Auckland, New Zealand

Received 25 September 2000; accepted 7 November 2000

Abstract

Reaction between $OsPhCl(CO)(PPh_3)_2$ and $HSi(OEt)_3$ gives the five-coordinate complex, $Os[Si(OEt)_3]Cl(CO)(PPh_3)_2$ (**1**), the crystal structure of which reveals a square pyramidal geometry with the triethoxysilyl ligand at the apical site and the two triphenylphosphine ligands arranged mutually *trans*. Addition of CO gives the six-coordinate complex, $Os[Si(OEt)_3]Cl(CO)_2(PPh_3)_2$ (**2**), but this addition is thermally reversible. The chloride ligand in **1** is replaced easily and reaction with LiR gives the stable, five-coordinate complexes, $Os[Si(OEt)_3]R(CO)(PPh_3)_2$ (**3a**, R = phenyl; **3b**, R = *o*-tolyl). Crystal structure determinations for **3a** and **3b** reveal a coordination geometry almost unchanged from that of **1** with Cl replaced by phenyl and *o*-tolyl, respectively. Addition of CO to **3a** and **3b** gives the six-coordinate complexes, $Os[Si(OEt)_3]R(CO)_2(PPh_3)_2$ (**4a**, R = phenyl) (**4b**, R = *o*-tolyl). Crystal structure determinations for **4a** and **4b** confirm octahedral geometry for each compound. Despite having adjacent aryl and silyl ligands neither **3a**, **3b** nor **4a**, **4b** show any tendency to undergo reductive elimination of $RSi(OEt)_3$. IR, ^1H-, ^{13}C- and ^{29}Si-NMR data for all new complexes are presented.

Keywords: Silyl complexes; Aryl complexes; Osmium; X-ray crystal structures

1. Introduction

C–Si bond formation, from reductive elimination of adjacent alkyl and silyl ligands in an alkyl, silyl–metal species, is widely postulated as the product-forming step in metal-catalyzed hydrosilation [1]. There have been studies of this process, both theoretical [2] and experimental, using isolable alkyl, silyl–platinum [3] and alkyl, silyl–palladium [4] complexes. Fewer studies have been made with octahedral metal complexes, but an important result was the demonstration that C–H and C–Si reductive elimination could be competitive for an iridium(III) complex containing hydride, alkyl, and silyl ligands [5]. In our studies of boryl (BR_2) complexes of osmium [6], we have recently demonstrated that when an aryl ligand is incorporated into the complex, and is adjacent to the boryl ligand, as in $Os(Bcat)R(CO)(PPh_3)_2$ and *cis*-$Os(Bcat)R(CO)_2(PPh_3)_2$, a very facile reductive elimination reaction occurs producing the borane $R–BR_2$ [7]. To examine whether or not, in a comparable coordination environment but with a silyl ligand replacing the boryl ligand, a similarly facile reductive elimination of the silane $R–SiR_3$ would occur, we needed to prepare suitable complexes incorporating both silyl and aryl ligands. We have previously described numerous five-coordinate silyl complexes of osmium(II) from reaction between $OsPhCl(CO)(PPh_3)_2$ and the appropriate silane [8]. For this work we chose the triethoxysilyl ligand, introduced by reaction with $HSi(OEt)_3$, because it is a tightly bound ligand and therefore offered a good chance for successful isolation of the sought after aryl, silyl–osmium complexes. In

* Corresponding author. Tel.: +64-9-3737999, ext. 8320; fax: +64-9-3737422.

E-mail address: w.roper@auckland.ac.nz (W.R. Roper).

0022-328X/01/$ - see front matter
PII: S0022-328X(00)00899-8

this paper we describe (i) the synthesis of five- and six-coordinate triethoxysilyl complexes of osmium(II) with a crystal structure of the five-coordinate complex, (ii) the introduction of aryl groups (phenyl and *o*-tolyl) into these complexes through reaction with lithium aryls, (iii) structural studies of both the five- and six-coordinate mixed silyl, aryl complexes, and (iv) preliminary observations of the reactivity of these compounds towards reductive elimination reactions.

2. Results and discussion

2.1. Preparation and crystal structure of $Os[Si(OEt)_3]Cl(CO)(PPh_3)_2$ (1)

The reaction between $OsPhCl(CO)(PPh_3)_2$ and $HSi(OEt)_3$ proceeds smoothly to produce $Os[Si(OEt)_3]Cl(CO)(PPh_3)_2$ (**1**) (see Scheme 1) as a yellow crystalline solid. The IR spectrum of **1** (see Table 1) shows a strong absorption at 1914 cm^{-1} (ν(CO)) and another at 1099 cm^{-1} characteristic of the triethoxysilyl ligand. The ^{1}H-NMR spectrum (see Table 2) of **1** reveals a triplet at 0.93 ppm ($^3J_{HH} = 7.0$ Hz) which is assigned to the methyl protons of the three ethyl groups. A quartet at 3.33 ppm ($^3J_{HH} = 7.0$ Hz) is assigned to the corresponding methylene groups. The ^{13}C-NMR spectrum (see Table 3) includes resonances for the ethyl groups at 17.7 and 57.9 ppm, as well as a triplet for the carbonyl carbon resonance at 182.1 ppm ($^2J_{CP} = 9$ Hz). The ^{29}Si-NMR spectrum (see Table 4) shows a triplet at -61.1 ppm ($^2J_{CP} = 11$ Hz), with coupling to two magnetically equivalent phosphorus nuclei. The $^{31}P\{^1H\}$ spectrum (see Table 5) shows a broad singlet at 23.6 ppm. All of the above spectroscopic data is compatible with the geometry depicted for **1** in Scheme 1, and to confirm this and to provide a point of reference for the structures to be discussed later in this paper, a crystal structure determination of **1** was completed.

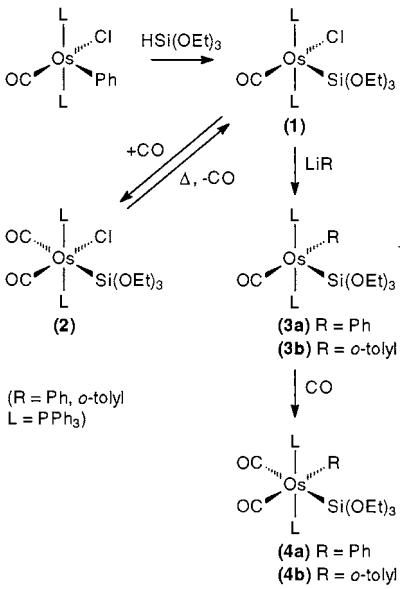

Scheme 1. Syntheses of aryl, triethoxysilyl complexes of osmium(II).

Table 1
IR data for osmium silyl complexes

Complex	ν(CO) (cm^{-1})	Other bands (cm^{-1})
$Os[Si(OEt)_3]Cl(CO)(PPh_3)_2$ (**1**)	1914	1099, 1070, 941
$Os[Si(OEt)_3]Cl(CO)_2(PPh_3)_2$ (**2**)	2013, 1947	1040, 936
$Os[Si(OEt)_3](Ph)(CO)(PPh_3)_2$ (**3a**)	1914	1108, 1094, 1073, 937
$Os[Si(OEt)_3](o\text{-tolyl})(CO)(PPh_3)_2$ (**3b**)	1916	1116, 1103, 1093, 1073, 938
$Os[Si(OEt)_3](Ph)(CO)_2(PPh_3)_2$ (**4a**)	2015, 1950	1116, 1101, 1090, 1070, 929
$Os[Si(OEt)_3](o\text{-tolyl})(CO)_2(PPh_3)_2$ (**4b**)	2005, 1945	1115, 1101, 1088, 1070, 938

The molecular geometry of **1** is illustrated in Fig. 1, while selected interatomic distances and bond angles are tabulated in Table 7. The structure has four independent molecules in the asymmetric unit. Like other five-coordinate silyl complexes of osmium(II) which we have studied [8] this compound has a square pyramidal geometry with the silyl group at the apical position. The Os–Si distance (2.319(2) Å, average of the four independent molecules) is identical to the distance found for $Os[Si(OH)_3]Cl(CO)(PPh_3)_2$ [8b] and very close to the value found for the silatranyl complex $Os(silatranyl)Cl(CO)(PPh_3)_2$ [8f] (2.326(2) Å). Other structural features for **1** are unremarkable.

2.2. Preparation of the six-coordinate triethoxysilyl complex, $Os[Si(OEt)_3]Cl(CO)_2(PPh_3)_2$ (2)

A solution of the unsaturated five-coordinate complex **1** decolourised rapidly when treated with carbon monoxide (see Scheme 1). The IR spectrum of the resulting colourless complex, $Os[Si(OEt)_3]Cl(CO)_2(PPh_3)_2$ (**2**), shows ν(CO) bands at 2013 and 1947 cm^{-1}. The ^{1}H- and ^{13}C-NMR spectra of **2** are very similar to those of **1** but the ^{29}Si-NMR spectrum (see Table 4) reveals a triplet at -19.5 ppm ($^2J_{SiP} = 18$ Hz), considerably shifted to higher frequency and with a larger coupling constant, relative to compound **1**. The values are, however, very close to those recorded for $Os[Si(OH)_3]Cl(CO)_2(PPh_3)_2$ (-10.6 ppm, t, $^2J_{SiP} = 18$ Hz) [9]. Surprisingly, and in marked contrast to the aryl, silyl derivatives described below, the CO addition is readily reversible both in solution and in the solid state. Solutions of **2** at room temperature over several hours become yellow with the formation of **1**.

Table 2
^{1}H-NMR data for osmium silyl complexes

Complex	^{1}H, δ (ppm)
Os[Si(OEt)$_3$]Cl(CO)(PPh$_3$)$_2$ (**1**)	0.93 (t, $J = 7.0$ Hz, 9H, OCH$_2$*Me*), 3.33 (q, $J = 7.0$ Hz, 6H, OC*H*$_2$Me), 7.36–7.96 (m, 30H, PPh$_3$).
Os[Si(OEt)$_3$]Cl(CO)$_2$(PPh$_3$)$_2$ (**2**)	0.91 (t, $J = 7.0$ Hz, 9H, OCH$_2$*Me*), 3.46 (q, $J = 7.0$ Hz, 6H, OC*H*$_2$Me), 7.33–7.71 (m, 30H, PPh$_3$).
Os[Si(OEt)$_3$](Ph)(CO)(PPh$_3$)$_2$ (**3a**)	0.91 (t, $J = 6.8$ Hz, 9H, OCH$_2$*Me*), 3.53 (q, $J = 6.8$ Hz, 6H, OC*H*$_2$Me), 6.56 (br s, 3H, Ph), 7.18–7.31 (m, 32H, 2H Ph, 30H PPh$_3$).
Os[Si(OEt)$_3$](*o*-tolyl)(CO)(PPh$_3$)$_2$ (**3b**)	Isomer 1: 0.34 (s, 3H, C$_6$H$_4$*Me*), 0.88 (t, $J = 6.9$ Hz, 9H, OCH$_2$*Me*), 3.36 (q, $J = 6.9$ Hz, 6H, OC*H*$_2$Me), 6.03 (d, $J = 7.1$ Hz, 1H, C$_6$*H*$_4$Me), 6.61 (t apparent, $J = 7.1$ Hz, 1H, C$_6$*H*$_4$Me), 6.67 (t apparent, $J = 7.1$ Hz, 1H, C$_6$*H*$_4$Me). Isomer 2: 0.95 (t, $J = 6.8$ Hz, 9H, OCH$_2$*Me*), 1.56 (s, 3H, C$_6$H$_4$*Me*), 3.59 (q, $J = 6.8$ Hz, 6H, OC*H*$_2$Me), 4.93 (d, $J = 7.2$ Hz, 1H, C$_6$*H*$_4$Me), 5.98 (t apparent, $J = 7.2$ Hz, 1H, C$_6$*H*$_4$Me), 6.45 (t apparent, $J = 7.2$ Hz, 1H, C$_6$*H*$_4$Me). Overlapping resonances of both isomers: 7.18–7.35 (m, PPh$_3$). Fourth phenyl proton obscured.
Os[Si(OEt)$_3$](Ph)(CO)$_2$(PPh$_3$)$_2$ (**4a**)	0.89 (t, $J = 6.8$ Hz, 9H, OCH$_2$C*H*$_3$), 3.36 (q, $J = 6.8$ Hz, 6H, OC*H*$_2$CH$_3$), 6.27 (t apparent, $J = 7.2$ Hz, 2H, Ph), 6.60 (t apparent, $J = 7.2$ Hz, 1H, Ph), 7.16–7.41 (m, 32H, 2H Ph, 30H PPh$_3$).
Os[Si(OEt)$_3$](*o*-tolyl)(CO)$_2$(PPh$_3$)$_2$ (**4b**)	0.90 (t, $J = 7.0$ Hz, 9H, OCH$_2$*Me*), 1.53 (s, 3H, C$_6$H$_4$*Me*), 3.33 (q, $J = 7.0$ Hz, 6H, OC*H*$_2$Me), 6.00 (t apparent, $J = 7.1$ Hz, 1H, C$_6$*H*$_4$Me), 6.46 (d, $J = 7.1$ Hz, 1H, C$_6$*H*$_4$Me), 6.57 (t apparent, $J = 7.1$ Hz, 1H, C$_6$*H*$_4$Me), 7.14 (m, 12H, PPh$_3$), 7.21 (m, 6H, PPh$_3$), 7.40 (m, 12H, PPh$_3$), 7.82 (d, $J = 7.1$ Hz, 1H, C$_6$*H*$_4$Me).

Table 3
^{13}C-NMR data for osmium silyl complexes

Complex	^{13}C, δ (ppm)
Os[Si(OEt)$_3$]Cl(CO)(PPh$_3$)$_2$ (**1**)	17.7 (OCH$_2$*Me*), 57.9 (O*C*H$_2$Me), 127.8 (t′ [11], $^{2,4}J_{CP} = 9$ Hz, *o*-PPh$_3$), 129.8 (s, *p*-PPh$_3$), 132.5 (t′, $^{1,3}J_{CP} = 50$ Hz, *i*-PPh$_3$), 134.8 (t′, $^{3,5}J_{CP} = 11$ Hz, *m*-PPh$_3$), 182.1 (t, $^2J_{CP} = 9$ Hz, CO).
Os[Si(OEt)$_3$]Cl(CO)$_2$(PPh$_3$)$_2$ (**2**)	17.9 (OCH$_2$*Me*), 58.1 (O*C*H$_2$Me), 127.5 (t′, $^{2,4}J_{CP} = 9$ Hz, *o*-PPh$_3$), 129.7 (s, *p*-PPh$_3$), 134.2 (t′, $^{3,5}J_{CP} = 11$ Hz, *m*-PPh$_3$), 134.7 (t′, $^{1,3}J_{CP} = 52$ Hz, *i*-PPh$_3$), 178.3 (t, $^2J_{CP} = 9$ Hz, CO), 178.7 (t, $^2J_{CP} = 8$ Hz, CO).
Os[Si(OEt)$_3$](Ph)(CO)(PPh$_3$)$_2$ (**3a**)	18.0 (OCH$_2$*Me*), 58.4 (O*C*H$_2$Me), 121.2 (br s, Ph), 127.6 (t′, $^{2,4}J_{CP} = 10$ Hz, *o*-PPh$_3$), 129.4 (s, *p*-PPh$_3$), 133.5 (t′, $^{1,3}J_{CP} = 48$ Hz, *i*-PPh$_3$), 134.7 (t′, $^{3,5}J_{CP} = 11$ Hz, *m*-PPh$_3$), 178.3 (t, $^2J_{CP} = 12$ Hz, CO), 193.8 (t, $^2J_{CP} = 8$ Hz, *i*-Ph). 2 signals for Os*Ph* not detected.
Os[Si(OEt)$_3$](*o*-tolyl)(CO)(PPh$_3$)$_2$ (**3b**)	Isomer 1: 17.9 (OCH$_2$*Me*), 23.3 (C$_6$H$_4$*Me*), 58.5 (O*C*H$_2$Me), 121.4 (*C*$_6$H$_4$Me), 125.4 (C$_6$*H*$_4$Me), 127.3 (t′, $^{2,4}J_{CP} = 9$ Hz, *o*-PPh$_3$), 128.3 (*C*$_6$H$_4$Me), 129.1 (s, *p*-PPh$_3$), 134.9 (t′, $^{3,5}J_{CP} = 11$ Hz, *m*-PPh$_3$), 141.8 (*C*$_6$H$_4$Me), 144.0 (*C*$_6$H$_4$Me), 178.6 (t, $^2J_{CP} = 12$ Hz, CO), 194.4 (t, $^2J_{CP} = 9$ Hz, *i*-*C*$_6$H$_4$Me). *ipso*-PPh$_3$ not detected. Isomer 2: 17.9 (OCH$_2$*Me*), 26.5 (C$_6$H$_4$*Me*), 58.8 (O*C*H$_2$Me), 119.8 (*C*$_6$H$_4$Me), 121.9 (*C*$_6$H$_4$Me), 127.3 (t′, $^{2,4}J_{CP} = 9$ Hz, *o*-PPh$_3$), 129.3 (s, *p*-PPh$_3$), 130.4 (*C*$_6$H$_4$Me), 131.4 (*C*$_6$H$_4$Me), 134.9 (t′, $^{3,5}J_{CP} = 11$ Hz, *m*-PPh$_3$), 149.2 (*C*$_6$H$_4$Me), 179.7 (t, $^2J_{CP} = 14$ Hz, CO), 193.7 (t, $^2J_{CP} = 8$ Hz, *i*-*C*$_6$H$_4$Me). *Ipso*-PPh$_3$ not detected.
Os[Si(OEt)$_3$](Ph)(CO)$_2$(PPh$_3$)$_2$ (**4a**)	18.0 (s, OCH$_2$*C*H$_3$), 58.4 (s, O*C*H$_2$CH$_3$), 121.0 (s, Ph), 125.9 (s, Ph), 127.0 (t′, $^{2,4}J_{CP} = 10$ Hz, *o*-PPh$_3$), 129.1 (s, *p*-PPh$_3$), 134.6 (t′, $^{3,5}J_{CP} = 10$ Hz, *m*-PPh$_3$), 134.8 (t′, $^{1,3}J_{CP} = 52$ Hz, *i*-PPh$_3$), 140.3 (t, $^2J_{CP} = 12$ Hz, *i*-Ph), 148.4 (s, Ph), 182.7 (t, $^2J_{CP} = 8$ Hz, *C*O), 185.4 (t, $^2J_{CP} = 7$ Hz, *C*O).
Os[Si(OEt)$_3$](*o*-tolyl)(CO)$_2$(PPh$_3$)$_2$ (**4b**)	17.9 (OCH$_2$*Me*), 31.8 (C$_6$H$_4$*Me*), 58.5 (O*C*H$_2$Me), 122.1 (*C*$_6$H$_4$Me), 123.7 (*C*$_6$H$_4$Me), 126.9 (t′, $^{2,4}J_{CP} = 9$ Hz, *o*-PPh$_3$), 127.5 (*C*$_6$H$_4$Me), 129.0 (s, *p*-PPh$_3$), 134.6 (t′, $^{3,5}J_{CP} = 10$ Hz, *m*-PPh$_3$), 135.1 (t′, $^{1,3}J_{CP} = 52$ Hz, *i*-PPh$_3$), 146.7 (t, $^2J_{CP} = 12$ Hz, *i*-*C*$_6$H$_4$Me), 149.0 (*C*$_6$H$_4$Me), 152.9 (*C*$_6$H$_4$Me), 183.7 (t, $^2J_{CP} = 8$ Hz, CO), 183.7 (t, $^2J_{CP} = 9$ Hz, CO).

Likewise, when solid **2** is heated at 125°C under vacuum CO is slowly lost and **1** is reformed.

2.3. Preparation and crystal structures of Os[Si(OEt)$_3$]R(CO)(PPh$_3$)$_2$ (**3a**, R = Ph; **3b**, R = *o*-tolyl)

Treatment of **1** with RLi (R = Ph, *o*-tolyl) results in displacement of the labile chloride ligand affording the five-coordinate silyl, aryl complexes, Os[Si(OEt)$_3$]-R(CO)(PPh$_3$)$_2$ (**3a**, R = Ph; **3b**, R = *o*-tolyl) (see Scheme

Table 4
^{29}Si-NMR data for osmium silyl complexes

Complex	^{29}Si, δ (ppm)
Os[Si(OEt)$_3$]Cl(CO)(PPh$_3$)$_2$ (**1**)	−61.1 (t, Os*Si*, $^2J_{SiP} = 11$)
Os[Si(OEt)$_3$]Cl(CO)$_2$(PPh$_3$)$_2$ (**2**)	−19.5 (t, Os*Si*, $^2J_{SiP} = 18$)
Os[Si(OEt)$_3$](Ph)(CO)(PPh$_3$)$_2$ (**3a**)	−68.1 (t, Os*Si*, $^2J_{SiP} = 14$)
Os[Si(OEt)$_3$](*o*-tolyl)(CO)(PPh$_3$)$_2$ (**3b**)	−66.7 (t, Os*Si*, $^2J_{SiP} = 14$), −73.5 (t, Os*Si*, $^2J_{SiP} = 15$)
Os[Si(OEt)$_3$](Ph)(CO)$_2$(PPh$_3$)$_2$ (**4a**)	−22.5 (t, Os*Si*, $^2J_{SiP} = 24$)
Os[Si(OEt)$_3$](*o*-tolyl)(CO)$_2$(PPh$_3$)$_2$ (**4b**)	−26.5 (t, Os*Si*, $^2J_{SiP} = 23$)

Table 5
^{31}P-NMR data for osmium silyl complexes

Complex	$^{31}P\{^1H\}$, δ (ppm)
$Os[Si(OEt)_3]Cl(CO)(PPh_3)_2$ (**1**)	23.6 (bs, Os*P*)
$Os[Si(OEt)_3]Cl(CO)_2(PPh_3)_2$ (**2**)	−12.4 (bs, Os*P*)
$Os[Si(OEt)_3](Ph)(CO)(PPh_3)_2$ (**3a**)	23.9 (bs, Os*P*)
$Os[Si(OEt)_3](o\text{-tolyl})(CO)(PPh_3)_2$ (**3b**)	22.7 (bs, Os*P*), 25.2 (bs, Os*P*)
$Os[Si(OEt)_3](Ph)(CO)_2(PPh_3)_2$ (**4a**)	−3.2 (s, Os*P*), with satellites (d, $^2J_{PSi} = 24$ Hz)
$Os[Si(OEt)_3](o\text{-tolyl})(CO)_2(PPh_3)_2$ (**4b**)	−5.3 (s, Os*P*), with satellites (d, $^2J_{PSi} = 23$ Hz)

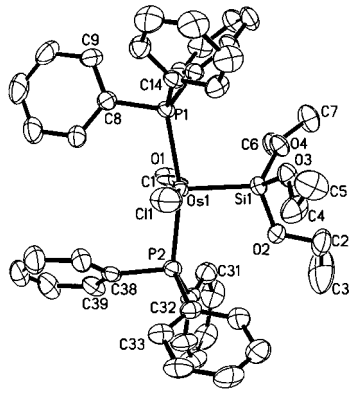

Fig. 1. Molecular geometry of $Os[Si(OEt)_3]Cl(CO)(PPh_3)_2$ (**1**).

1) in good yield. The analogous transformations also occur readily for the corresponding boryl complex, $Os(Bcat)Cl(CO)(PPh_3)_2$ [7]. **3a** and **3b** are bright orange crystalline solids with good stability both in the solid state and in solution. In the IR spectra of both of these compounds the ν(CO) values (see Table 1) are almost unchanged from the value found for **1**. The NMR spectroscopic data (see Tables 2–5) for **3a** are as expected, however all NMR data for **3b** is indicative of the presence of two isomers. This same phenomenon

Table 6
Data collection and processing parameters

	1	**3a**	**3b**	**4a**	**4b**
Formula	$C_{43}H_{45}ClOsP_2Si$	$C_{49}H_{50}O_4OsP_2Si$	$C_{50}H_{52}O_4OsP_2Si$	$C_{50}H_{50}O_5OsP_2Si$	$C_{51}H_{52}O_5OsP_2Si$
Molecular weight	941.47	983.12	997.15	1011.13	1025.16
T (K)	200	150	200	150	200
Wavelength (Å)	0.71073	0.71073	0.71073	0.71073	0.71073
Crystal system	Triclinic	Monoclinic	Monoclinic	Orthorhombic	Monoclinic
Space group	$P\bar{1}$	$P2_1/c$	$P2_1/c$	$P2_12_12_1$	$P2_1/n$
a (Å)	10.3380(2)	10.7412(2)	19.6526(2)	12.3458(1)	13.9740(1)
b (Å)	22.1043(4)	32.0669(6)	12.5130(1)	15.7999(2)	22.4592(1)
c (Å)	37.0723(8)	13.2119(3)	20.7190(1)	22.8179(3)	14.3258(1)
α (°)	78.025(1)				
β (°)	82.736(1)	106.918(1)	117.600(1)		94.240(1)
γ (°)	88.803(1)				
V (Å^3)	8220.6(3)	4353.72(15)	4515.16(5)	4450.19(9)	4483.78
Z	8	4	4	4	4
D_{calc} (g cm^{-3})	1.521	1.500	1.467	1.509	1.519
$F(000)$	3776	1984	2016	2040	2072
μ (mm^{-1})	3.32	3.07	2.96	3.01	2.990
Crystal size mm	$0.42 \times 0.20 \times 0.12$	$0.16 \times 0.14 \times 0.12$	$047 \times 0.40 \times 0.35$	$0.60 \times 0.12 \times 0.08$	$0.36 \times 0.16 \times 0.14$
2θ (min–max) (°)	1.0–28.2	1.7–26.3	1.2–27.4	1.6–27.1	1.7–25.0
h, k, l range	$-13 \le h \le 13$, $-27 \le k \le 27$, $0 \le l \le 48$	$-13 \le h \le 12$, $0 \le k \le 40$, $0 \le l \le 16$	$-25 \le h \le 22$, $0 \le k \le 16$, $0 \le l \le 25$	$-15 \le h \le 15$, $0 \le k \le 19$, $0 \le l \le 28$	$-16 \le h \le 16$, $0 \le k \le 26$, $0 \le l \le 17$
Reflections collected	80912	24945	41889	26961	50098
Independent reflections	36062 $R_{int} = 0.0418$	8784 $R_{int} = 0.0283$	10023 $R_{int} = = 0.0228$	9452 $R_{int} = 0.0264$	7881 $R_{int} = 0.0328$
A (min–max)	0.336, 0.692	0.639, 0.709	0.336, 0.423	0.265, 0.795	0.412, 0.679
Function minimised	$\Sigma w(F_o^2 - F_c^2)^2$	$\Sigma w(F_o^2 - F_c^2)^2$	$\Sigma w(F_o^2 - F_c^2)^2$	$\Sigma w(F_o^2 - F_c^2)^2$	$\Sigma w(F_o^2 - F_c^2)^2$
Goodness-of-fit on F^2	1.089	1.103	1.122	1.045	1.149
R (observed data) [a]	$R_1 = 0.0544$, $wR_2 = 0.1157$	$R_1 = 0.0272$, $wR_2 = 0.0569$	$R_1 = 0.0283$, $wR_2 = 0.0607$	$R_1 = 0.0243$, $wR_2 = 0.0519$	$R_1 = 0.0378$, $wR_2 = 0.0854$
R (all data)	$R_1 = 0.0788$, $wR_2 = 0.1263$	$R_1 = 0.0337$, $wR_2 = 0.0594$	$R_1 = 0.0342$, $wR_2 = 0.0641$	$R_1 = 0.0299$, $wR_2 = 0.0545$	$R_1 = 0.0535$, $wR_2 = 0.0958$
Diff. map (min–max) (e Å^{-3})	+2.96, −1.75	+1.15, −0.71	+1.36, −0.65	+1.05, −0.89	+2.15, 1.10

[a] $R = \Sigma||F_o| - |F_c||/\Sigma|F_o|$, $wR_2 = \{\Sigma[w(F_o^2 - F_c^2)^2]/\Sigma[w(F_o^2)^2]\}^{1/2}$.

Table 7
Selected bond lengths (Å) and bond angles (°) for **1**

	Molecule 1	Molecule 2	Molecule 3	Molecule 4
Bond lengths				
Os–C(1)	1.924(7)	1.939(7)	1.922(7)	1.910(7)
Os–Si	2.3311(18)	2.317(2)	2.3166(18)	2.312(2)
Os–P(1)	2.3778(17)	2.3823(17)	2.3835(16)	2.3787(17)
Os–P(2)	2.3666(17)	2.3850(17)	2.3889(17)	2.3630(16)
Os–Cl	2.433(3)	2.423(3)	2.438(3)	2.431(3)
Si–O(2)	1.652(5)	1.617(7)	1.629(6)	1.627(6)
Si–O(3)	1.655(5)	1.652(5)	1.651(5)	1.642(5)
Si–O(4)	1.651(5)	1.657(7)	1.657(5)	1.685(6)
Bond angles				
C(1)–Os–Si	94.7(3)	95.0(3)	94.1(3)	90.9(2)
C(1)–Os–P(1)	86.7(2)	90.1(2)	89.6(2)	86.7(2)
C(1)–Os–P(2)	91.7(2)	93.0(2)	92.6(2)	91.8(2)
C(1)–Os–Cl	163.5(3)	159.0(3)	160.2(3)	163.7(2)
Si–Os–P(1)	98.34(6)	96.52(7)	95.15(6)	97.77(7)
Si–Os–P(2)	97.34(6)	96.36(7)	95.36(6)	97.15(7)
Si–Os–Cl	101.78(8)	105.96(10)	105.71(8)	105.32(9)
Cl–Os–P(1)	89.91(7)	85.84(7)	86.91(7)	86.73(7)
Cl–Os–P(2)	87.17(7)	86.59(7)	87.45(7)	90.52(8)
P(1)–Os–P(2)	164.31(6)	166.44(6)	169.10(6)	165.03(6)

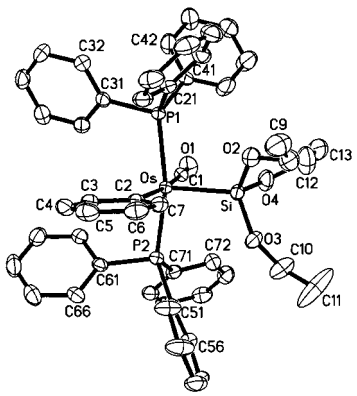

Fig. 2. Molecular geometry of $Os[Si(OEt)_3](Ph)(CO)(PPh_3)_2$ (**3a**).

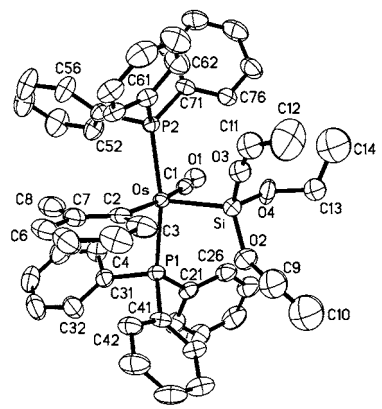

Fig. 3. Molecular geometry of $Os[Si(OEt)_3](o\text{-tolyl})(CO)(PPh_3)_2$ (**3b**).

was also observed for the five-coordinate *o*-tolyl, boryl complex, $Os(Bcat)(o\text{-tolyl})(CO)(PPh_3)_2$ [7]. We believe the two isomers are rotational isomers arising from

Table 8
Selected bond lengths (Å) and bond angles (°) for **3a**

Bond lengths	
Os–C(1)	1.899(4)
Os–C(2)	2.147(3)
Os–Si	2.3218(9)
Os–P(2)	2.3577(8)
Os–P(1)	2.3796(8)
Si–O(3)	1.643(2)
Si–O(4)	1.650(3)
Si–O(2)	1.666(3)
Bond angles	
C(1)–Os–C(2)	171.21(13)
C(1)–Os–Si	87.35(10)
C(2)–Os–Si	101.24(9)
C(1)–Os–P(2)	91.23(10)
C(2)–Os–P(2)	89.70(8)
Si–Os–P(2)	96.10(3)
C(1)–Os–P(1)	89.93(10)
C(2)–Os–P(1)	87.22(8)
Si–Os–P(1)	96.90(3)
P(2)–Os–P(1)	166.98(3)

Table 9
Selected bond lengths (Å) and bond angles (°) for **3b**

Bond lengths	
Os–C(1)	1.879(3)
Os–C(2)	2.161(3)
Os–Si	2.3258(9)
Os–P(1)	2.3671(8)
Os–P(2)	2.3782(8)
Si–O(3)	1.616(5)
Si–O(2)	1.643(3)
Si–O(4)	1.649(3)
Si–O(3)′	1.698(6)
Bond angles	
C(1)–Os–C(2)	169.88(14)
C(1)–Os–Si	87.37(10)
C(2)–Os–Si	102.76(11)
C(1)–Os–P(1)	91.33(10)
C(2)–Os–P(1)	88.00(9)
Si–Os–P(1)	93.14(3)
C(1)–Os–P(2)	88.64(10)
C(2)–Os–P(2)	89.85(8)
Si–Os–P(2)	99.27(3)
P(1)–Os–P(2)	167.58(3)

restricted rotation of the *o*-tolyl ligand. It is worth noting that the chemical shifts for the *o*-tolyl methyl protons are quite different in the two rotamers (0.34 and 1.56 ppm) reflecting very different environments for these methyl groups. The ^{13}C-NMR data reveals that in both isomers the two triphenylphosphine ligands are mutually trans and the chemical shifts for the CO ligands are closely similar. Both these observations support rotational rather than stereo-isomers. Furthermore, no isomers are observed for the six-coordinate di-carbonyl derivative, $Os[Si(OEt)_3](o\text{-tolyl})(CO)_2(PPh_3)_2$ (**4b**), where restricted rotation of

the *o*-tolyl ligand is less likely because of the increased Os–Si, Os–P, and Os–C(*o*-tolyl) distances (see Tables 9 and 11 and discussion of the structures below).

The solid state geometries of **3a** and **3b**, obtained by X-ray crystallography, are depicted in Figs. 2 and 3, and selected bond lengths and bond angles are presented in Tables 8 and 9, respectively. The geometries of both are closely similar to that of **1** with phenyl or *o*-tolyl replacing the chloride ligand. It is interesting that in these complexes, where there are two ligands, aryl and silyl, of recognised strong σ-bonding/*trans* influence character, it is the silyl ligand which dominates and which adopts the apical site of the square pyramid. The phenyl and *o*-tolyl ligands are approximately coplanar with the plane through the Os, Si, and C(1) atoms and the Si–Os–C(2) angles are effectively the same (**3a**, 101.24(9)°; **3b**, 102.76(11)°). The Si–Os–C(1) angles are also identical and slightly less than 90° (**3a**, 87.35(10)°; **3b**, 87.37(10)°). The Os–Si distances are also very similar and little changed from the value in **1** (**3a**, 2.3218(9)°; **3b**, 2.3258(9)°). The same is true of the Os–P and Os–C distances (see Tables 8 and 9).

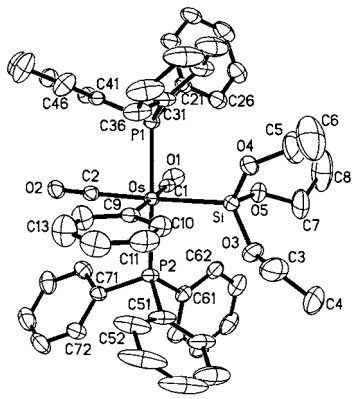

Fig. 4. Molecular geometry of $Os[Si(OEt)_3](Ph)(CO)_2(PPh_3)_2$ (**4a**).

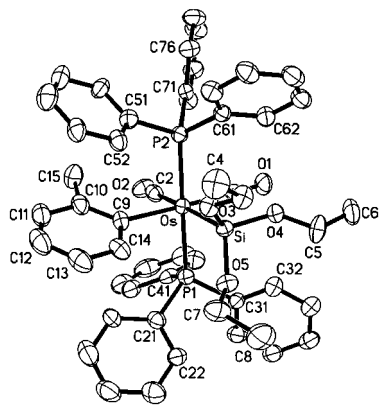

Fig. 5. Molecular geometry of $Os[Si(OEt)_3](o\text{-tolyl})(CO)_2(PPh_3)_2$ (**4b**).

Table 10
Selected bond lengths (Å) and bond angles (°) for **4a**

Bond lengths	
Os–C(1)	1.921(3)
Os–C(2)	1.934(3)
Os–C(9)	2.175(3)
Os–P(2)	2.4058(8)
Os–P(1)	2.4079(8)
Os–Si	2.4906(10)
Si–O(3)	1.659(3)
Si–O(4)	1.660(3)
Si–O(5)	1.676(3)
Bond angles	
C(1)–Os–C(2)	91.26(14)
C(1)–Os–C(9)	178.20(13)
C(2)–Os–C(9)	86.97(14)
C(1)–Os–P(2)	92.45(12)
C(2)–Os–P(2)	91.73(10)
C(9)–Os–P(2)	87.28(10)
C(1)–Os–P(1)	92.30(12)
C(2)–Os–P(1)	88.33(10)
C(9)–Os–P(1)	87.98(10)
P(2)–Os–P(1)	175.25(4)
C(1)–Os–Si	88.76(10)
C(2)–Os–Si	178.16(10)
C(9)–Os–Si	93.01(9)
P(2)–Os–Si	90.11(3)
P(1)–Os–Si	89.83(3)

Table 11
Selected bond lengths (Å) and bond angles (°) for **4b**

Bond lengths	
Os–C(1)	1.904(6)
Os–C(2)	1.947(6)
Os–C(9)	2.220(5)
Os–P(1)	2.4109(13)
Os–P(2)	2.4145(13)
Os–Si	2.4804(14)
Si–O(4)	1.649(4)
Si–O(3)	1.658(4)
Si–O(5)	1.661(4)
Bond angles	
C(1)–Os–C(2)	90.4(2)
C(1)–Os–C(9)	177.1(2)
C(2)–Os–C(9)	92.1(2)
C(1)–Os–P(1)	91.60(15)
C(2)–Os–P(1)	86.85(15)
C(9)–Os–P(1)	90.03(13)
C(1)–Os–P(2)	89.24(15)
C(2)–Os–P(2)	96.46(15)
C(9)–Os–P(2)	89.00(13)
P(1)–Os–P(2)	176.58(5)
C(1)–Os–Si	86.81(16)
C(2)–Os–Si	174.89(16)
C(9)–Os–Si	90.88(14)
P(1)–Os–Si	88.97(5)
P(2)–Os–Si	87.77(4)

2.4. Preparation and crystal structures of $Os[Si(OEt)_3]R(CO)_2(PPh_3)_2$ (**4a**, R = Ph; **4b**, R = *o*-tolyl)

Both **3a** and **3b** react readily with CO to form the corresponding colourless, six-coordinate, di-carbonyl complexes, $Os[Si(OEt)_3]R(CO)_2(PPh_3)_2$ (**4a**, R = Ph; **4b**, R = *o*-tolyl) (see Scheme 1). Whereas addition of CO to **1** is reversible, neither **4a** nor **4b** show any tendency to lose CO. The mutually cis arrangement of the two CO ligands is confirmed by the appearance of two ν(CO) bands in the IR spectra. The ^{1}H- and ^{13}C-NMR spectroscopic data are as expected and there is no evidence for the existence of isomers for the *o*-tolyl complex, **4b**. The ^{29}Si resonances of the five-coordinate complexes **1**, **3a**, and **3b**, all move to higher frequency on addition of CO to form **2**, **4a**, and **4b**, respectively, whereas the ^{31}P resonances move to lower frequency.

The solid state geometries of **4a** and **4b**, obtained by X-ray crystallography, are depicted in Figs. 4 and 5, and selected bond lengths and bond angles are presented in Tables 10 and 11, respectively. Both compounds have regular octahedral geometry about osmium with mutually *trans* triphenylphosphine ligands and mutually cis CO ligands. All bond lengths to osmium increase upon changing from the five-coordinate geometry of **3a** and **3b** to the six-coordinate geometry of **4a** and **4b**. The most striking increase involves the Os–Si distances which increase by up to 0.17 Å (**3a**, 2.3218(9), **4a**, 2.4906(10); **3b**, 2.3258(9), **4b**, 2.4804(14)). Increases in the Os–P and Os–C distances are less but still significant (see Tables 10 and 11).

4a and **4b** are thermally robust as solids and in solution. In contrast to the *cis*-boryl, aryl complexes, $Os(Bcat)R(CO)_2(PPh_3)_2$ [7], which readily undergo reductive elimination of R–Bcat in solution with accompanying formation of '$Os(CO)_2(PPh_3)_2$' (as the *ortho*-metallated isomer), complexes **4a** and **4b** are reluctant to eliminate R–$Si(OEt)_3$ even under forcing conditions (see Section 4). Thus, **4a** and **4b** do not model the Si–C bond-forming step proposed in metal catalysed hydrosilation.

3. Conclusions

Five-coordinate mixed silyl, aryl complexes of osmium(II) have been prepared by treating $Os[Si(OEt)_3]Cl(CO)(PPh_3)_2$ with lithium aryls. In previous studies we have shown that the five-coordinate complexes, $Os(BR_2)Cl(CO)(PPh_3)_2$ [7], $Os(SiR_3)Cl(CO)(PPh_3)_2$ [8], and $OsRCl(CO)(PPh_3)_2$ [10] adopt a square pyramidal geometry with the boryl, silyl, and R groups, respectively, in the apical position. In this study the accessibility of $Os(SiR_3)R(CO)(PPh_3)_2$ presents the opportunity to examine whether or not the square pyramidal geometry is still retained and if so which of these two strong trans influence ligands, silyl or aryl, occupies the apical site. Structural study confirms that it is the silyl ligand. Unlike the mixed boryl, aryl complexes of osmium(II), neither $Os[Si(OEt)_3]R(CO)(PPh_3)_2$ nor $Os[Si(OEt)_3]R(CO)_2(PPh_3)_2$ undergo ready reductive elimination of R–$Si(OEt)_3$.

4. Experimental

4.1. General procedures and instruments

Standard laboratory procedures were followed as have been described previously [11]. The compound $OsPhCl(CO)(PPh_3)_2$ was prepared according to the literature method [10].

Infrared spectra (4000–400 cm^{-1}) were recorded as Nujol mulls between KBr plates on a Perkin–Elmer Paragon 1000 spectrometer. NMR spectra were obtained on a Bruker DRX 400 at 25°C. ^{1}H-, ^{13}C-, ^{31}P- and ^{29}Si-NMR spectra were obtained operating at 400.1 (^{1}H), 100.6 (^{13}C), 162.0 (^{31}P), and 79.5 (^{29}Si) MHz, respectively. Resonances are quoted in ppm and ^{1}H-NMR spectra referenced to either tetramethylsilane (0.00 ppm) or the proteo-impurity in the solvent (7.25 ppm for $CHCl_3$). ^{13}C-NMR spectra were referenced to $CDCl_3$ (77.0 ppm), ^{31}P-NMR spectra to 85% orthophosphoric acid (0.0 ppm) as an external standard, and ^{29}Si-NMR spectra to tetramethylsilane (0.0 ppm). Mass spectra were recorded using the fast atom bombardment technique with a Varian VG 70-SE mass spectrometer. Elemental analyses were obtained from the Microanalytical Laboratory, University of Otago.

4.2. Preparation of $Os[Si(OEt)_3]Cl(CO)(PPh_3)_2$ (**1**)

$OsCl(Ph)(CO)(PPh_3)_2$ (200 mg, 0.234 mmol) and $HSi(OEt)_3$ (52 μl, 0.28 mmol) were heated under a nitrogen atmosphere in toluene (25 ml) for 2 h. The solvent was removed in vacuo, and the resulting yellow residue was dissolved in dichloromethane (25 ml). This solution was filtered through a Celite pad and ethanol (10 ml) was added. The dichloromethane was removed on the rotary evaporator to yield bright-yellow crystals that were recrystallised from dichloromethane:ethanol (25:10 ml) to give pure **1** (193 mg, 86%). *m*/*z* 905.2184; $C_{43}H_{45}O_4OsP_2Si$ [$M^{+\bullet} - Cl$] requires 905.2147. Anal. Calc. for $C_{43}H_{45}ClO_4OsP_2Si$: C, 54.85; H, 4.82. Found: C, 54.15; H, 5.03%.

4.3. Preparation of $Os[Si(OEt)_3]Cl(CO)_2(PPh_3)_2$ (**2**)

$Os[Si(OEt)_3]Cl(CO)(PPh_3)_2$ (200 mg, 0.212 mmol) was dissolved in dichloromethane (20 ml), and the

solution introduced to a Fischer–Porter bottle and treated with carbon monoxide (4 atm.). Ethanol (10 ml) was added to the resulting colourless solution and the dichloromethane was removed to yield colourless crystals of pure complex **2** (183 mg, 89%). m/z 935.2130; $C_{44}H_{45}O_5OsP_2Si$ $[M^{+\bullet} - Cl]$ requires 935.2126. Anal. Calc. for $C_{44}H_{45}ClO_5OsP_2Si$: C, 54.50; H, 4.67. Found: C, 54.06; H, 4.94%.

4.4. Preparation of Os[Si(OEt)$_3$](Ph)(CO)(PPh$_3$)$_2$ (3a)

To a yellow solution of Os[Si(OEt)$_3$]Cl(CO)(PPh$_3$)$_2$ (108 mg, 0.115 mmol) in benzene (15 ml) at 5°C was added a solution of LiPh in Et_2O (0.83 M, 0.17 ml, 0.14 mmol), giving a bright orange, cloudy solution. The mixture was allowed to warm up to room temperature and was stirred for a further 30 min. Concentration of the solution in vacuo to about 3 ml and addition of hexane gave a bright orange precipitate of pure **3a** which was collected on a glass frit and washed with EtOH and hexane (65 mg, 58%). Anal. Calc. for $C_{49}H_{50}O_4OsP_2Si$: C, 59.86; H, 5.13. Found: C, 59.82; H, 5.24%.

4.5. Preparation of Os[Si(OEt)$_3$](o-tolyl)(CO)(PPh$_3$)$_2$ (3b)

To a yellow solution of Os[Si(OEt)$_3$]Cl(CO)(PPh$_3$)$_2$ (298 mg, 0.317 mmol) in benzene (25 ml) at 5°C was added a solution of Li-*o*-tolyl in Et_2O (0.75 M, 0.55 ml, 0.413 mmol) giving a bright orange cloudy solution. The mixture was allowed to warm up to room temperature and was stirred for a further 30 min. Concentration of the solution in vacuo to about 3 ml and addition of hexane gave a bright orange precipitate of pure **3b** which was collected on a glass frit and washed with EtOH and hexane (284 mg, 90%). Anal. Calc. for $C_{50}H_{52}O_4OsP_2Si$: C, 60.22; H, 5.26. Found: C, 60.05; H, 5.16%.

4.6. Preparation of Os[Si(OEt)$_3$](Ph)(CO)$_2$(PPh$_3$)$_2$ (4a)

A stream of CO gas was passed through a solution of Os[Si(OEt)$_3$](Ph)(CO)(PPh$_3$)$_2$ (120 mg, 0.122 mmol) in benzene (5 ml) for 30 s, generating a pale yellow solution. Concentration of the solution in vacuo to about 1 ml followed by addition of hexane gave a white precipitate which was collected on a glass frit and washed with EtOH and hexane. The product was recrystallised from benzene/hexane to give pure **4a** (102 mg, 82%). Anal. Calc. for $C_{50}H_{50}O_5OsP_2Si$: C, 59.39; H, 4.98. Found: C, 59.35; H, 5.13%.

4.7. Preparation of Os[Si(OEt)$_3$](o-tolyl)(CO)$_2$(PPh$_3$)$_2$ (4b)

A stream of CO gas was passed through a solution of Os[Si(OEt)$_3$](*o*-tolyl)(CO)(PPh$_3$)$_2$ (100 mg, 0.100 mmol) in benzene (12 ml) for 20 s, generating a pale yellow solution. Concentration of the solution in vacuo to about 1 ml followed by addition of hexane gave a white precipitate which was collected on a glass frit and washed with EtOH and hexane. This product was recrystallised from CH_2Cl_2/EtOH to give pure **4b** (91 mg, 89%). Anal. Calc. for $C_{51}H_{52}O_5OsP_2Si$: C, 59.75; H, 5.11. Found: C, 59.70; H, 5.23%.

4.8. Thermolysis of Os[Si(OEt)$_3$](Ph)(CO)$_2$(PPh$_3$)$_2$ (4a) and Os[Si(OEt)$_3$](o-tolyl)(CO)$_2$(PPh$_3$)$_2$ (4b)

Unchanged **4a** was recovered in high yield from solutions of **4a** in toluene which had been heated to 75°C for 2 h. At higher temperatures in toluene some decomposition occurred over two hours but neither $PhSi(OEt)_3$ nor *ortho*-metallated '$Os(CO)_2(PPh_3)_2$' could be detected amongst the products.

Heating solid samples of **4b** under vacuum at 125°C for 24 h resulted in loss of CO only to give **3b** quantitatively. Further heating of solid samples of **3b** under vacuum at 125°C for 48 h returned **3b** unchanged.

4.9. X-ray crystal structure determinations for complexes 1, 3a, 3b, 4a and 4b

X-ray data collection was on a Siemens SMART diffractometer with a CCD area detector, using graphite monochromated Mo–K_α radiation ($\lambda =$ 0.71073 Å). Data were integrated and Lorentz and polarisation correction applied using SAINT [12] software. Semi-empirical absorption corrections were applied based on equivalent reflections using SADABS [13]. The structures were solved by Patterson and Fourier methods and refined by full-matrix least squares on F^2 using programs SHELXS [14] and SHELXL [15]. All non-hydrogen atoms were refined anisotropically and hydrogen atoms were included in calculated positions and refined with a riding model with thermal parameter 20% greater than U_{iso} of the carrier atom. **1** has four independent molecules in the unit cell. Some of these show disorder in the phenyl carbon atoms consistent with rotation about the P–C bond. Crystal data and refinement details are given in Table 6.

5. Supplementary material

Crystallographic data for the structural analysis have been deposited with the Cambridge Crystallographic

Data Centre, CCDC nos. 149641–149645 for compounds **1**, **3a**, **3b**, **4a**, **4b**, respectively. Copies of this information may be obtained from The Director, CCDC, 12 Union Road, Cambridge CB2 1EZ, UK (fax: +44-1233-336033; e-mail: deposit@ccdc.cam.ac.uk or www: http://www.ccdc.cam.ac.uk).

Acknowledgements

We thank the Marsden Fund, administered by the Royal Society of New Zealand, for supporting this work and for granting Postdoctoral Fellowships to AW and MA. We also thank the University of Auckland Research Committee for partial support of this work through grants-in-aid and through the award of a Doctoral Scholarship to SDW.

References

[1] A.J. Chalk, J.F. Harrod, J. Am. Chem. Soc. 87 (1965) 16.
[2] S. Sakaki, N. Mizoe, M. Sugimoto, Organometallics 17 (1998) 2510.
[3] K. Hasebe, J. Kamite, T. Mori, H. Katayama, F. Ozawa, Organometallics 19 (2000) 2022.
[4] Y. Tanaka, H. Yamashita, S. Shimada, M. Tanaka, Organometallics 16 (1997) 3246.
[5] (a) M. Aizenberg, D. Milstein, Angew. Chem. Int. Ed. Engl. 33 (1994) 317. (b) U. Schubert, Angew. Chem. Int. Ed. Engl. 33 (1994) 419. M. Aizenberg, D. Milstein, J. Am. Chem. Soc. 117 (1995) 6456.
[6] (a) G.J. Irvine, M.J.G. Lesley, T.B. Marder, N.C. Norman, C.R. Rice, E.G. Robins, W.R. Roper, G.R. Whittell, L.J. Wright, Chem. Rev. 98 (1998) 2685. (b) G.R. Clark, G.J. Irvine, C.E.F. Rickard, W.R. Roper, A. Williamson, L.J. Wright, Boryl complexes of ruthenium and osmium, in: M.G. Davidson, A.K. Hughes, T.B. Marder, K. Wade (Eds.), Contemporary Boron Chemistry, Royal Society of Chemistry, Cambridge, 2000, p. 379.
[7] (a) C.E.F. Rickard, W.R. Roper, A. Williamson, L.J. Wright, Angew. Chem. Int. Ed. Engl. 38 (1999) 1110. (b) C.E.F. Rickard, W.R. Roper, A. Williamson, L.J. Wright, Organometallics, 19 (2000) 4344.
[8] (a) G.R. Clark, C.E.F. Rickard, W.R. Roper, D.M. Salter, L.J. Wright, Pure Appl. Chem. 62 (1990) 1039. (b) C.E.F. Rickard, W.R. Roper, D.M. Salter, L.J. Wright, J. Am. Chem. Soc. 114 (1992) 9682. (c) C.E.F. Rickard, W.R. Roper, D.M. Salter, L.J. Wright, Organometallics 11 (1992) 3931. (d) K. Hübler, W.R. Roper, L.J. Wright, Organometallics 16 (1997) 2730. (e) K. Hübler, P.A. Hunt, S.M. Maddock, C.E.F. Rickard, W.R. Roper, D.M. Salter, P. Schwerdtfeger, L.J. Wright, Organometallics 16 (1997) 5076. (f) M.T. Attar-bashi, C.E.F. Rickard, W.R. Roper, L.J. Wright, S.D. Woodgate, Organometallics 17 (1998) 504.
[9] W.R. Roper, D.M. Salter, L.J. Wright, unpublished work.
[10] C.E.F. Rickard, W.R. Roper, G.E. Taylor, J.M. Waters, L.J. Wright, J. Organomet. Chem. 389 (1990) 375.
[11] S.M. Maddock, C.E.F. Rickard, W.R. Roper, L.J. Wright, Organometallics 15 (1996) 1793.
[12] SAINT, Area detector integration software, Siemens Analytical Instruments Inc., Madison, WI, 1995.
[13] G.M. Sheldrick, SADABS, Program for semi-empirical absorption correction, University of Göttingen, 1977.
[14] G.M. Sheldrick, SHELXS, Program for crystal structure determination, University of Göttingen, 1977.
[15] G.M. Sheldrick, SADABS, Program for crystal structure refinement, University of Göttingen, 1977.